4. EXPERIMENTAL FACILITIES IN BEAM HALL

4.1 GENERAL PURPOSE SCATTERING CHAMBER (GPSC)

M. Archunan, Golda K. S., A. Kothari, P. Barua, P. Sugathan and R.K. Bhowmik

The major developmental activity carried out last year is the installation of new detector cooling system using glycol as the coolant. The compressor is kept close to the chamber to achieve better cooling. It was used in an experiment to cool four silicon surface barrier detectors simultaneously to about - 4oC. The new system is faster than the earlier one and it also has a warming up facility which enables warming up of the detector mounts to the room temperature in 20 minutes of time period.

A variety of experiments were carried out using this facility in different fields such as Nuclear Physics, Materials Science ant Atomic Physics. The list of experiments carried out last year using this facility is given below.

Nuclear & Atomic Physics Experiments

User	***Experiment***	***Beam***	***No of shifts***
Punjab Univ.	Study of induced fusion-fission dynamics	F (Pulsed)	15
VECC	Neutron flow in orbiting reaction	F	3
IUAC	Facility test	Fe	3

Materials Science Experiments

User	***Title***	***Beam***	***No of shifts***
Tezpur University	Application of SHI induced ion tracks for nanodevices	Cl	2
Kurukshetra Univ.	Development and characterization of Nano/micro structures	Si Ni	2
S.N.College, Kerala	Thermo responsible ion track membrane from elastomers for drug-release application	Au	2
Kurukshetra Univ.	Development and characterization of Nano/micro structures	Si Ni	2

Rajasthan University	Ion transport through track-etched polymeric membrane	Ag Cl	2
ISRO	Heavy ion induced effects in VLSL Devices	Si, Cl, Ti, Ni, Ag	2
Tezpur University	Investigation of energy and fluence dependence of SHI irradiation on ionic transport in polymer electrolytes	O	2
Pune University	Formation of nano sized electronic devices in polymers through SHI irradiation	Ni Si	2
Bangalore University	Study of semiconductor materials and devices using nuclear techniques	Li	3

4.1.1 Present Status of National Array of Neutron Detectors (NAND)

Golda K.S., R.P. Singh, Hardev Singh[1] , B. Behera[1], S. Mandal[2], Mihir Chatterjee, J. Zacharias, Venkataramanan, Arti Gupta, Rajesh Kumar, Ranjit[2], M. Archunan, A. Kothari, P. Barua, A Jhingan, P. Sugathan, S.K. Datta and R.K. Bhowmik

[1]Panjab University, Chandigargh.

[2]Delhi University, New Delhi.

This facility in the phase II beam hall consists of 30 neutron detectors at present. The set up is ready in all aspects to carry out experiments [1]. All beam line components are aligned and placed. Fig. 1 shows the reaction chamber with gas detectors, charged particle detectors and other accessories. Proper arrangements are done to transport signals from neutron detectors as well as other detectors like MWPCs and charged particle detectors placed inside chamber to the electronics area. A compact NIM based dual channel electronics module is developed in house to take care of all the electronic processing requirements of individual neutron detectors [2]. A CAMAC based data acquisition system is installed for multi parameter data collection.

REFERENCES

[1] K. S. Golda, et.al., DAE-BRNS- Symposium on Nucl. Physics, 2006, 626

[2] S. Venkataramanan, et.al., DAE-BRNS- Symposium on Nucl. Physics, 2006, 606

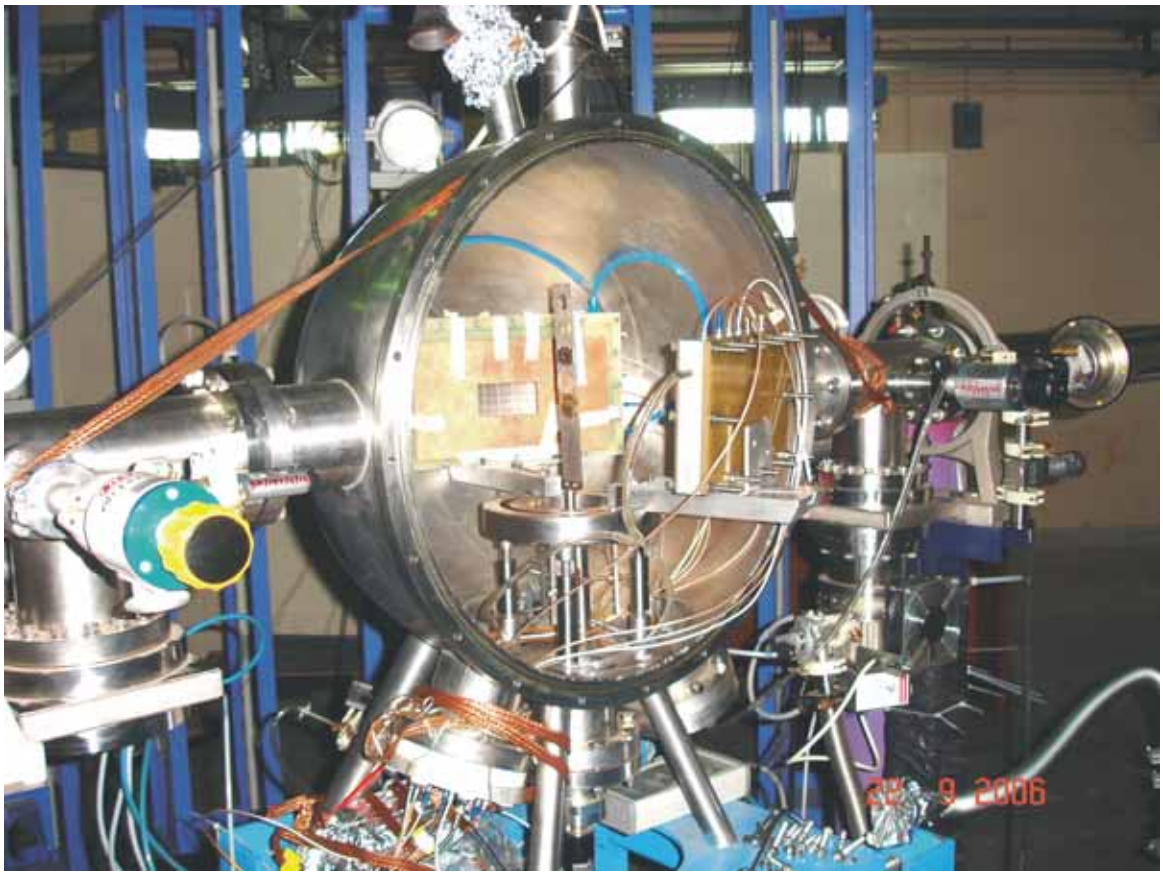

Fig. 1. Reaction Chamber with targets and detectors inside.

4.1.2 First Experiment with NAND for Studies on Fusion-Fission Reaction Dynamics

Golda K.S., Hardev Singh[1], R.P. Singh, A Jhingan, P. Sugathan, Sunil[2], Bhavana[2], Ranjit[2], Anukul Dhal[3], Pravin Kumar[4] and R.K Bhowmik

[1]Panjab University, Chandigargh.
[2]Delhi University, New Delhi.
[3]Banarus Hindu university, Banarus
[4]Karnataka University, Dharwad

A feasibility run has been carried out to study fusion-fission reaction dynamics using neutron array set up. Our interest was to study the nuclear orientation dependence on quasi-fission versus fusion-fission by neutron multiplicity measurements. 148MeV $^{28}Si^{10+}$ beam from Tandem-LINAC combination was put on 250 μg/cm^2 thick self supporting ^{181}Ta target to measure pre-and post-scission neutron multiplicities and fission fragment angular and mass distribution. Fission fragments were detected in two large area position sensitive MWPCs placed at folding angle. Fission detectors placed at a distance of 19cm had an average angular coverage of 30^o each. Two monitor

detectors, 300 μm thick silicon surface barrier, kept at $\pm 16^0$ were used for beam flux normalization purpose and on-line monitoring of beam phase and time. Neutron time of flights were measured in 16 neutron detectors placed at a distance of 2m from target around the scattering chamber in a cylindrical shape. Schematics of the experimental set up is shown in fig. 1.

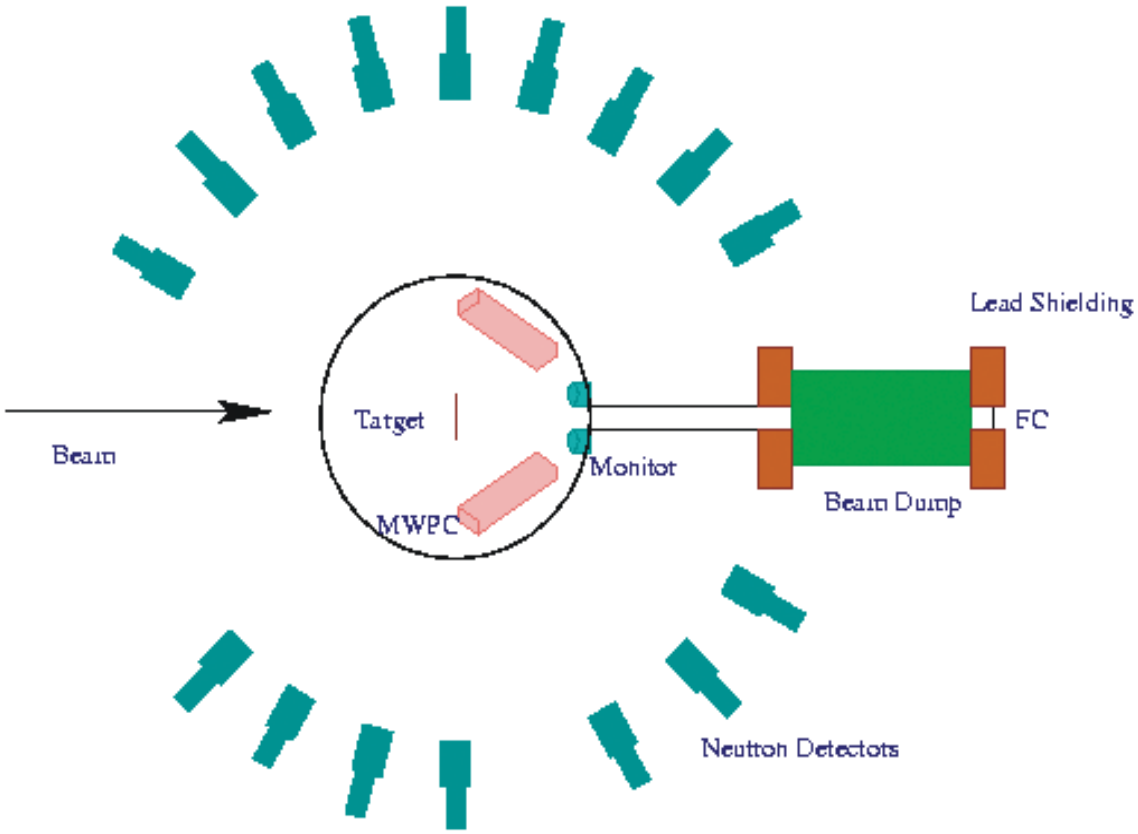

Fig. 1. Schematics of the experimental set-up

Pulsed beam with a repetition rate of 250ns enabled a good neutron gamma separation at 2meter flight path. Beam was dumped in borated paraffin shielded Ta Faraday cup 4.5 m down stream from the target. Time of Flight (TOF) method was used to measure the energy of neutrons as well as the velocity of fission fragments. RF signal from the beam buncher was used as the time reference. For coincidence between any neutron detectors with any fission fragment detectors, the arrival times for neutrons and fission fragments were recorded with respect to the timing signal from the beam buncher. Neutron TOF spectra was collected by setting a cutoff of neutron energy of about 0.5MeV by measuring the maximum Compton electron recoil energy using different gamma ray sources. Pulse shape discrimination technique was adapted for discriminating gamma rays detected by neutron detectors (Fig 2). CAMAC based data acquisition system was used to collect 60-parameter list mode data.

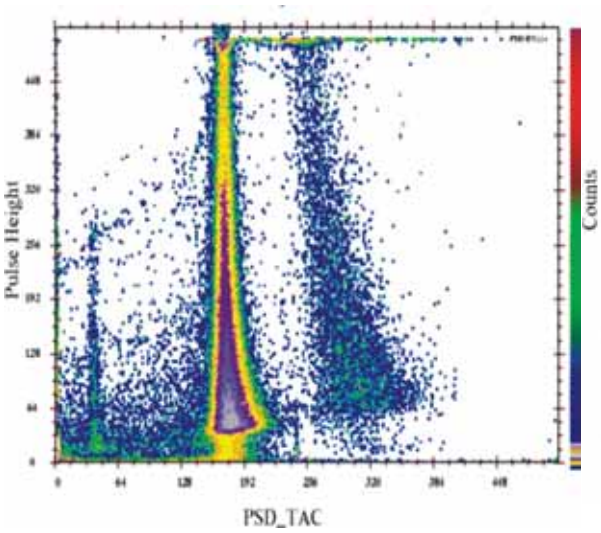

Fig.2. PSD_TAC vs. Pulse height obtained by home made electronics module.

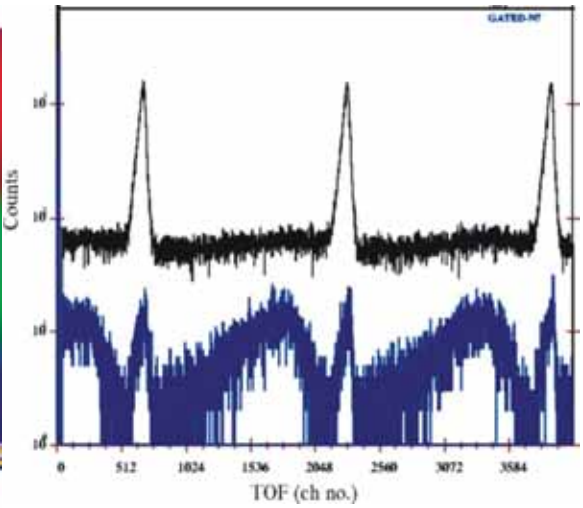

Fig. 3. TOF spectra are shown with (Blue line) and without (black line) PSD gating

The masses of the fission fragments were obtained from the angle and time of flight (TOF) information measured using MWPCs assuming no particle evaporation from the compound nucleus. The time correlation between two complementary fission fragments is shown in fig 3. The electronic delay between the two MWPC time signals was determined by assuming symmetric mass distribution of fission fragments.

The extracted mass distribution of fission fragments in the reaction $^{28}Si + ^{181}Ta$ @ 148 MeV with Gaussian fit is given in fig. 4. Since RF signal from the beam buncher is taken as the time reference for TOF measurements, the mass resolution is mainly limited by the beam pulse width (~ 2 ns).

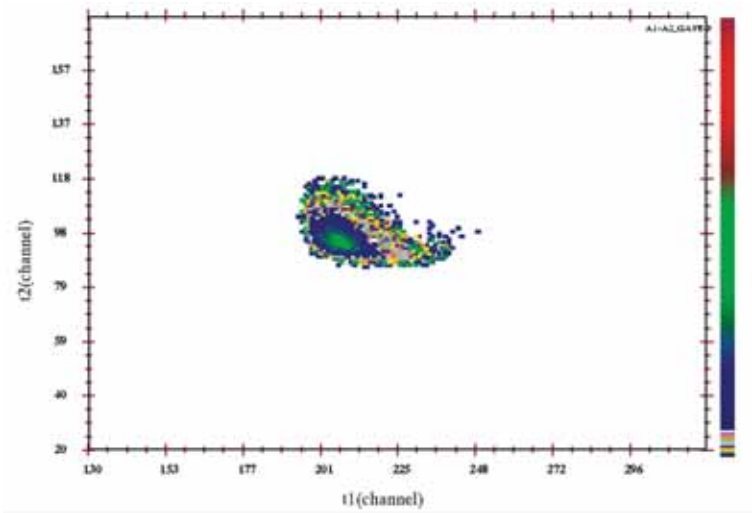

Fig. 3 .Time correlation between two complimentary fragments

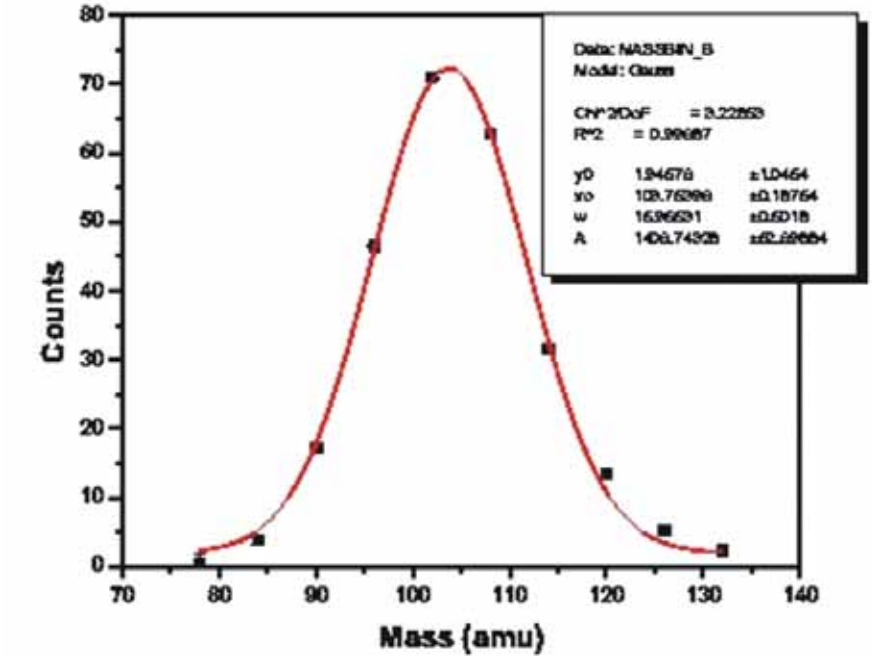

Fig. 4. Mass distribution of fission fragments in the reaction $^{28}Si + ^{181}Ta$ @ 148 MeV

4.2 GAMMA DETECTOR ARRAY (GDA)

V. Kumar, D. Negi, Kusum Rani, Rakesh Kumar, R.P.Singh, S.Muralithar, and R.K.Bhowmik

4.2.1 Experiments using GDA related facilities

The GDA facilities were used in this year for a variety of studies like nuclear structure at high spins, measurement of lifetime and electromagnetic moments and the studies of reaction mechanism like incomplete fusion, fission hindrance and entrance channel effects. There were in total ten number of experiments were done (refer table).

Description	Beam	Energy MeV	Shifts	User	Facility
Fission Fusion dynamics	^{19}F	82-125	24	Praveen/KU	HIRA/BGO
Isomers of n rich nuclei in A~208	^{19}F	117.5	3	AKS/UGC-DAE-CSR	HIRA/Ge
Spectroscopy of ^{141}Nd	^{16}O	68-92	13	GG / CU	GDA

Study of Transfer-Fission excitation	^{40}Ca	106-146	18	SM/DU	HPGe
Magnetic rotation - Odd isotopes Rb	^{7}Li	36	12	PB/SINP	GDA
High Spin ^{134,135}Ba	^{9}Be	42.5	15	Suresh / IITR	GDA
Lifetime of ^{75}Br states	^{51}Cr	150	18	DN/IUAC	GDA / RDD
Incomplete Fusion study	^{16}O	90	15	AA/AMU	GDA/CPDA
Incomplete Fusion study	^{12}C	54-90	15	PPS/AMU	GDA/CPDA
Nuclear Structure A=120-130 region	^{11}B	55-62	18	DM/PU	GDA

4.2.2 HPGe detector Service / Annealing

As the Clover and HPGe detectors have been used continuously over the years they need periodic thermal treatment for the annealing of neutron induced damage. Eight detectors were evacuated while four detectors were annealed to restore their FWHM. Annealing cum evacuation facility was also used for SiLi detector of Panjab University and LEGe of Atomic Physics Group for recovering their detectors.

4.2.3 Indian National Gamma Array (INGA)

An experimental facility for studying nuclear spectroscopy at high spin and excitation energy is currently being set up at the beam Hall II of IUAC. The funding for this project has been provided by the Department of Science and Technology under the Indian national gamma Array project (INGA). The mechanical structure for mounting a set of Clover detectors with anti-Compton shields in precise orientations has been designed. The set of 24 ACS are mounted on two movable platforms on precision guide rails. The orientations of the different ACS are to be reproducible with an accuracy of 0.5^0 with respect to the three axes and their positions reproducible to an accuracy of 0.5 mm with respect to the target position. An overall view of the setup is shown in fig 1. Fig 2 shows the view from the side and fig 3 the view from the front.

The 4000 mm long guide rails with spacing of 1350 mm are to be embedded in the concrete floor so that they are precisely aligned along the beam line. The platforms can move on the rails so that their positions can be reproduced with an accuracy of 0.5 mm in all three directions. For Recoil-tagged Spectroscopy, the front half of the structure is removed and the back-half moved forward by ~ 2 meter.

The new Clover detectors along with Anti-Compton shields have arrived and have been tested for energy and time resolution. Including the old detectors, IUAC has now a total number of eight Compton-suppressed Clover detectors. The support structure which houses 24 number of Clover Germanium detectors with Anti-Compton Shield, with precision movement provision on rail, has been ordered. Six additional slots are available for the mounting of LEPS or neutron detectors. The fabrication and installation is expected to be completed in six months period. The procurement of components for setting up of beam line, detectors / electronics have started. The required number of ADC814, Clover electronics INGA Modules, High Voltage power supplies of Anti Compton Shields and Clover Germanium detectors and preamplifier power supplies are taken up by our in house personnel.

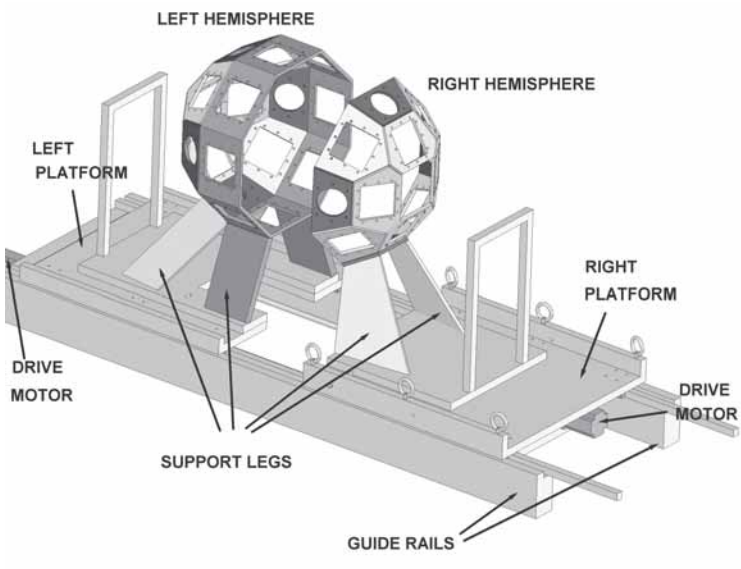

Fig. 1: View of the INGA structure in the beam hall

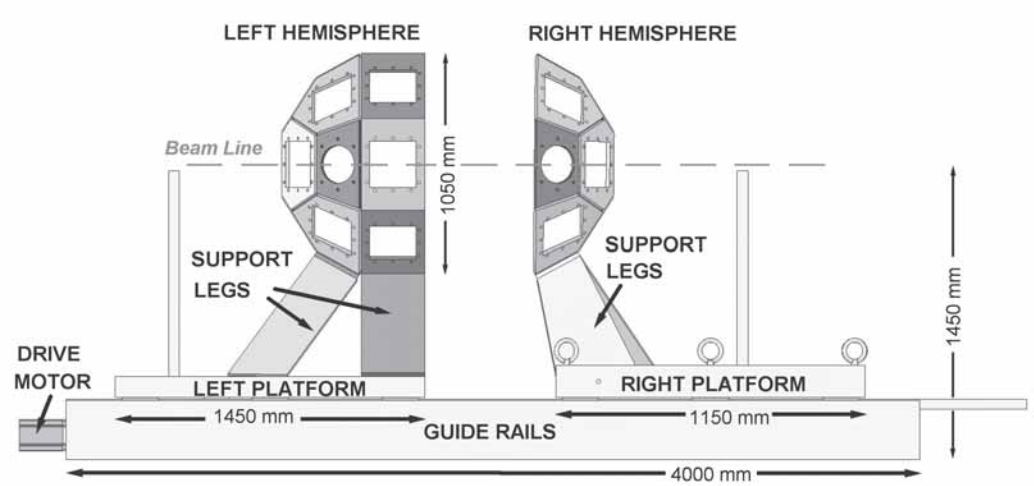

Fig. 2. INGA side view

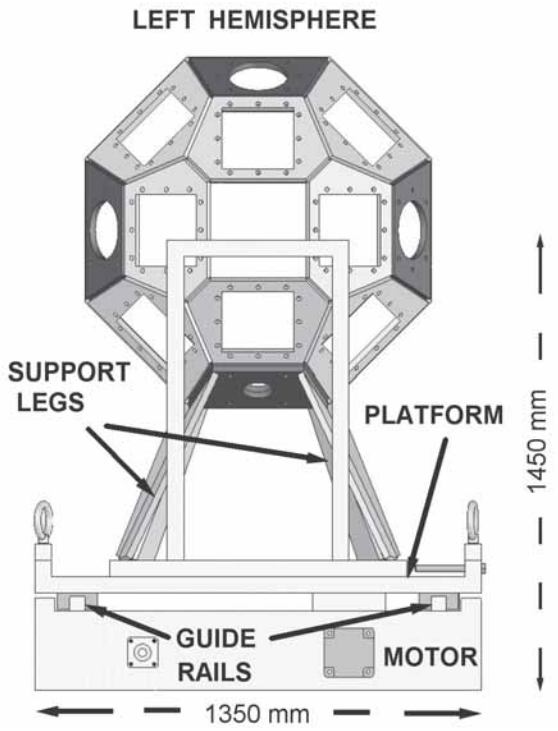

Fig. 3: INGA -front view

4.2.4 Clover Timing Measurement

S.Muralithar, S. Venkataramanan and R.K. Bhowmik

The timing measurements from in beam experiment (^{28}Si beam of 130 MeV on ^{100}Mo target) done in INGA-HIRA campaign was analyzed to minimize the electronics time delays. One time to Amplitude conversion spectrum (TAC) from two specific clover germanium detectors (number 7 and 8) was projected under the condition that only those two clover detectors should have fired and only specific crystals (one to four) of each detector should have valid energy data. It is observed that the timing (centroid and FWHM of different TAC's) can be different by as much as 15 ns depending on

(1) which clovers have fired (Fig 1)

(2) which crystals in each clover have fired (Fig 2)

(3) crystal fold (1 hit, 2 hit...) of the event (Fig 3) fired in each clover.

Precaution has to be taken while doing lifetime measurement (in few nano-second region) by properly correcting these time delays from detector / crystal combinations. These delays are primarily due to the mismatch of preamplifiers of different crystals in a Clover detector. We have plans to match the time delays in INGA clover modules of IUAC and dedicate one specific module for each clover.

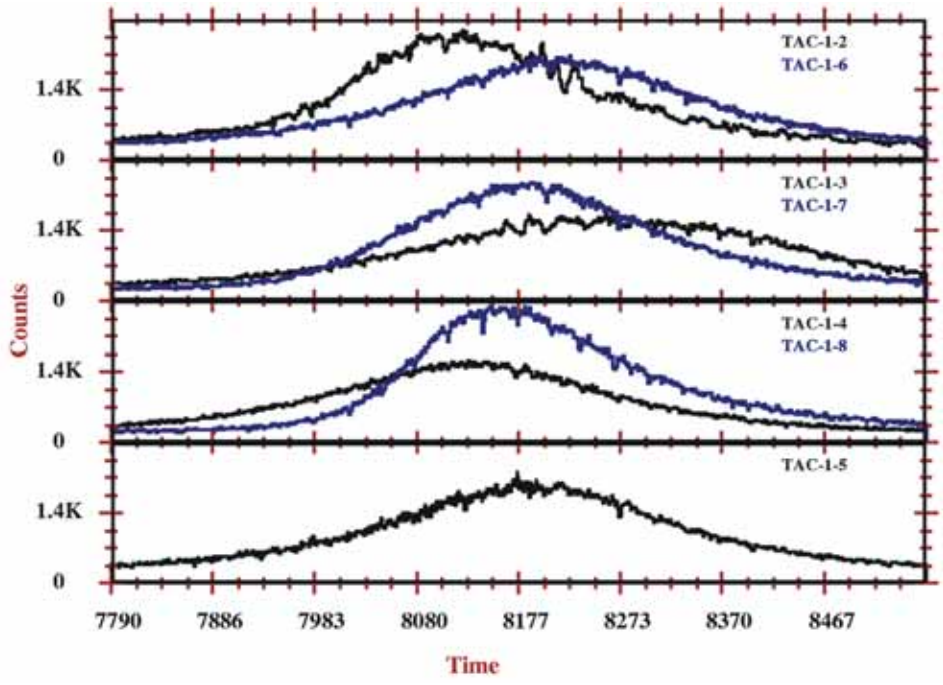

Fig.1 TAC spectra from different clover combinations

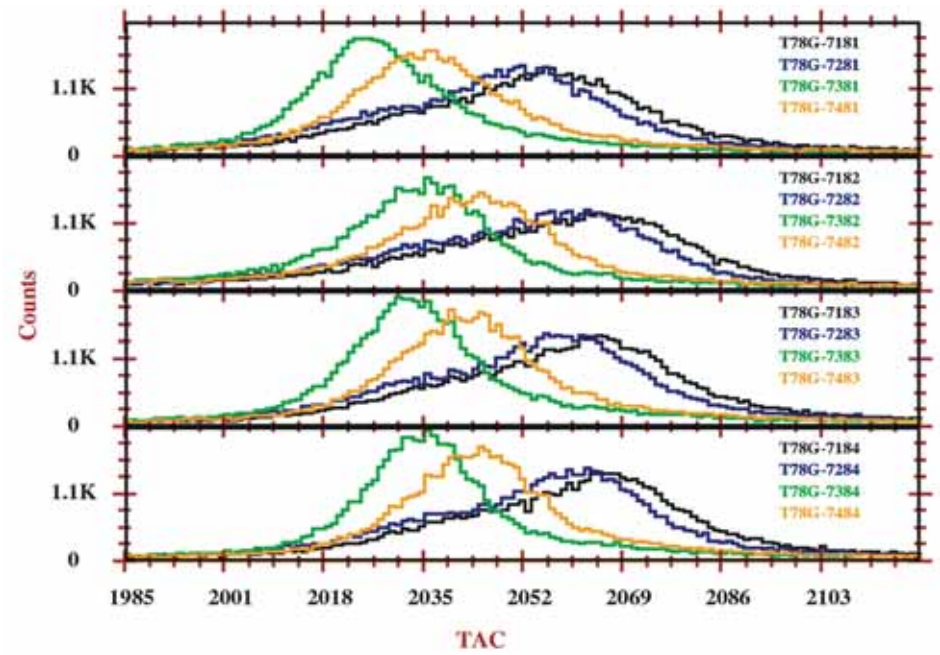

Fig. 2: TAC spectra from different crystals combination in a clover

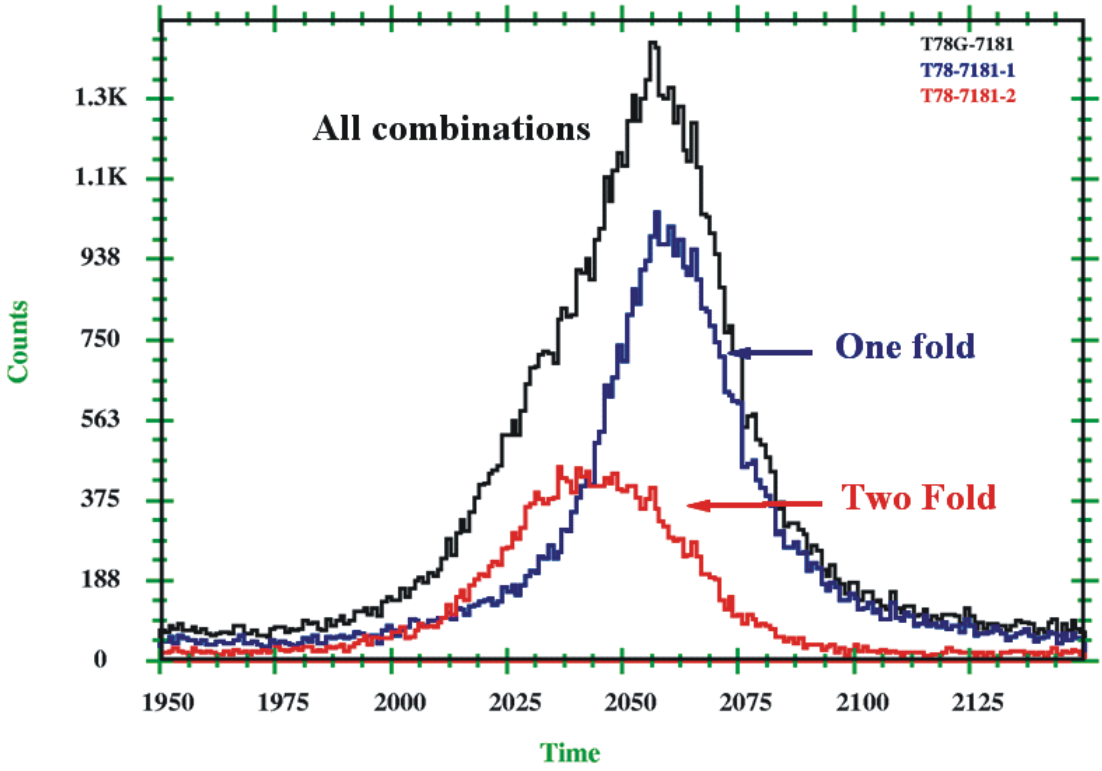

Fig. 3: TAC spectra from different crystal fold in a clover

4.2.5 New Recoil Distance Device for INGA

A new recoil distance device (plunger) for lifetime measurement is being constructed at IUAC. The plunger is designed to be used in conjunction with the Indian National Gamma Array (INGA) in the stand alone mode or in conjunction with the new mass spectrometer HYRA. The plunger will have three DC micrometers controlled by a PC. The details of the motors were given last year. The control program for the motors runs on a windows platform. The basic performance of the motors was tested. The chamber for the plunger would be made out of glass cylinder. The vacuum sealing will be through Wilson seals to the adapter aluminum flanges.

4.2.6 A new Spherical Shell Model program

J. A. Sheikh[1], R.P. Singh and R.K. Bhowmik

[1]University of Kashmir

One of the most challenging problems in nuclear physics is to study the structure of complex nuclei using the basic spherical shell model approach. This basic model provides a unified description of all the possible excitation modes of nuclei. Further, in the spherical shell model approach the inherent symmetries are preserved at each and every stage of the calculation.

Recently, a completely new spherical shell model program has been developed jointly by the Inter-University Accelerator Center and the University of Kashmir, Srinagar. There are only three to four such programs available in the world. This program works in the j-scheme. The main advantage of this program will be that it can be tailored to satisfy the needs of the nuclear physics community of the country. We have used this program to study the behavior of T=0 and T=1 pairing as a function of spin and temperature in the sd-shell region /1/. We are also using this program for the study of high spin states in the nuclei in sd-shell region with different interactions. In the lighter region of the periodic table, the dimensions of the matrices are of the order of 10^4 and can be solved using a Pentium-IV machine. With the availability of large computing facilities, it will now be possible to study even the deformed nuclei e.g, ^{76}Sr and others where we need to diagonalise matrices of dimension the order of 10^{10}.

REFERENCE

'Shell model study of pairing correlations' J. A. Sheikh et al; submited to Phys. Rev. C.

4.2.7 NP-LINAC 2006

One workshop on 'Nuclear Physics with LINAC Beam at IUAC' was held on Sept 14-15, 2006. Experimental proposals using the Beam hall II Nuclear Physics facilities (HYRA, INGA, NAND) were invited from current users. This resulted in a large number of experiment proposals from users across the country. These proposals were discussed in the December 2006 AUC workshop for allocation of beam time.

4.3 RECOIL MASS SPECTROMETERS

4.3.1 Heavy Ion Reaction Analyzer (HIRA)

J. Gehlot, S. Nath, A. Jhingan, T. Varughese, J. J. Das, P. Sugathan, N. Madhavan, GDA Group, P. Shidling[1] and Ranjeet[2]

[1]Department of Physics, Karnatak University, Dharwad, Karnataka
[2]Department of Physics and Astrophysics, Delhi University, Delhi

During this period, HIRA was used in two experiments involving stable beam and mass dispersive mode. The new focal plane detector system of HIRA was utilized in one of the experiments and was found to work well.

The last run of a student thesis experiment looking for fission hindrance in ^{19}F + ^{181}Ta --> ^{200}Pb*, populating the same compound nucleus as studied in a previous run using ^{16}O + ^{184}W [1] was carried out with HIRA + 14 BGO detectors. The beam rejection was excellent for this system too as shown in Fig. 1 (a) and (b), the first showing the ERs with ^{181}Ta target and HIRA set for 195 amu ERs and the second is for ^{197}Au target but with no change in the HIRA fields. The measured cross-section and moments of spin are being compared, for the second system, with theoretical calculations. The fusion excitation function and moments of the spin distribution for the two systems in

reduced co-ordinates show some effect of entrance channel (details are given elsewhere in this report by P. Shidling et al.).

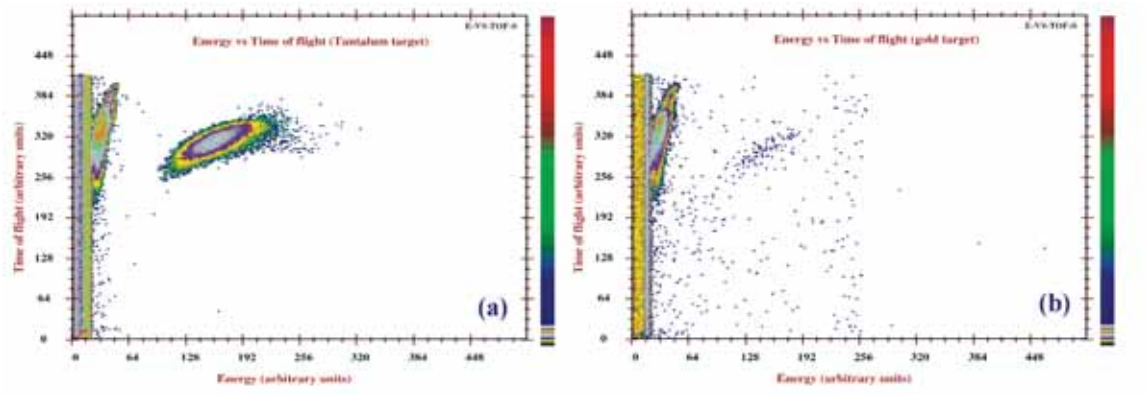

Fig. 1. Plot of E vs. TOF for (a) ^{181}Ta target and HIRA set for 195 amu mass and (b) for ^{197}Au target and same field setting showing negligible beam contamination (< 0.2 %)

The other thesis experiment (Delhi Univ.), related to transfer and fusion excitation function for ^{40}Ca + ^{66,70}Zn, was taken up in HIRA facility with the new large area MWPC detector (for position, timing and to some extent energy loss) followed by a split-anode ionization detector (for energy loss and residual energy of ions). Transfer was attempted at 5^{o} with respect to beam direction but the scattered beam-like particles falling on the large focal plane detector made it impossible to get Z-resolution and restricted data-taking. However, the fusion excitation function, angular distribution and transmission efficiency (of HIRA for ERs) measurements could be completed for ^{40}Ca + ^{70}Zn system. The use of two monitors, at identical angles on either side to start with, helped in proper normalization of cross-section during rotation of HIRA. Though the detector plate was held by the stationary entrance beam-port and independent of sliding seal chamber, some minor rotations in the plate during HIRA rotation could be taken care of, as the total angle subtended by the detectors at the target centre was always the same. Partial rotation of detector plate, during rotation of HIRA, could be detected and quantified too. Normalization with $(M1.M2)^{1/2}$ rather than (M1 + M2)/2 was used to prevent large errors, as in the past, where M1 and M2 are the counts in the elastic peaks detected in the two monitor detectors. Efficiency of HIRA was measured to be ~ 8 % for ERs from this system which is found to agree well with the values obtained with our simulation program [2]. Prior to this experiment, the electrostatic dipoles of HIRA were conditioned to +/- 181.5 kV in order to bend the transfer products of large E/q value, comfortably.

REFERENCES

[1]. P. Shidling et al., PRC 74 (2006) 064603

[2]. S. Nath et al., Section 4.3.3, NSC Annual Report 2004-2005

4.3.2 HYbrid Recoil mass Analyzer (HYRA)

N. Madhavan, S. Nath, T. Varughese, J. Gehlot, A. Jhingan, P. Sugathan, J. J. Das, A. K. Sinha[1], R. Singh[2], K. M. Varier[3], M. C. Radhakrishna[4], T.S.Datta, Jacob Chacko, P. Barua, Archunan, U. G. Naik, A. J. Malyadri, Beam transport group and GDA group

[1]IUC-DAE Consortium for Scientific Research, Kolkata Centre, Kolkata
[2]Department of Physics and Astrophysics, University of Delhi, Delhi
[3]Department of Physics, Calicut University, Kerala
[4]Department of Physics, Bangalore University, Bangalore

Status of stage I:

The first stage of HYRA QQ-MD-Q-MD has been commissioned in beam hall II at IUAC. Cooling water and electrical connections have been completed and found to be working satisfactorily. Beam-line has been laid and aligned. A long, 4" diameter beam-pipe is used at present in the region of planned INGA detector assembly. This will be suitably modified to take care of INGA and HYRA requirements, during the commissioning of INGA assembly. At present, a rolled nickel foil of 20 mm diameter and ~ 1.25 mg/cm^2 thickness is used as the pressure window for gas-filled mode operation, upstream of the target.

The power supplies have been connected to the magnets and tested at full power. The rise in temperature of the cooling water is found to be within expected limits. IGOR modules are being developed indigenously for remote control/read-back of power supply settings.

The movable stopper assembly, to be installed in Q3 to stop the various charge states of primary beam in vacuum mode of operation, is designed and some parts have been procured. Efforts are on to get it ready in the next few months. The focal plane chamber, for use with gas-filled mode, is being fabricated. A set-up for mounting a movable detector at Q3 centre is made which will allow optimization of gas-filled mode operation stage-wise.

Beam tests:

Two beam tests have been carried out using manual re-setting of power supplies, which is possible only after switching off the beam.

In the first test with beam, a 100 MeV ^{16}O beam was used on ~ 250 μg/cm^2 ^{184}W target (the effective energy of the beam on the target was about 97 MeV). Apart from checking the alignment of the beam-line, some data could be taken with focal plane detector. HYRA was initially operated in vacuum. The various charge states of beam-like particles but with same E/q reached the focal plane detector (a 5 cm x 5 cm, position sensitive resistive silicon detector). The beam rejection was of the order of 4 x 10^6. From the energy calibration of the detector one could ascertain the charge states of beam-like particles to be 4$^+$ to 7$^+$ of increasing yields (Fig. 1). On filling HYRA with 0.5 Torr of helium gas and setting the fields for charge equilibrated ERs, the originally detected beam-like particles were removed effectively

(due to larger bending, mainly in MD1 and to some extent in MD2) and lowest charge states (1^+ and 2^+) were found to reach the focal plane (Fig. 2). There was also an increased beam rejection factor of 10^9.

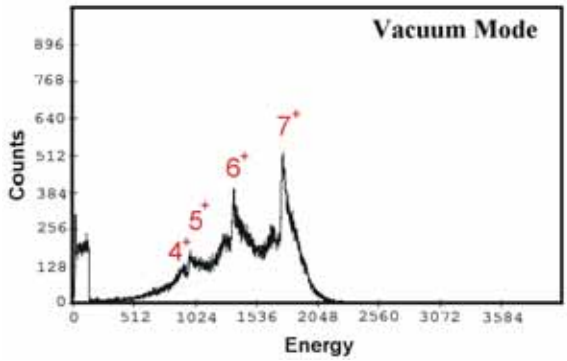

Fig. 1 : Vacuum mode energy spectrum showing 4^+ to 7^+ charge states of ^{16}O

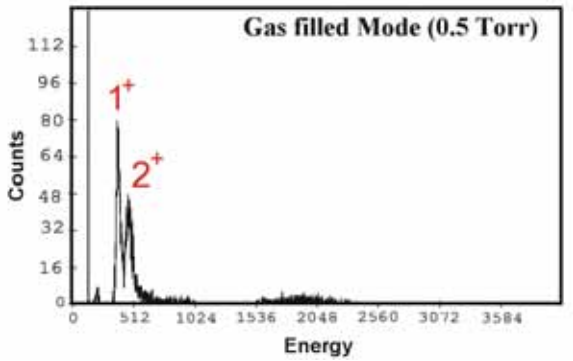

Fig 2 : Gas-filled mode (He~0.5 Torr) showing 1^+ and 2^+ charge states of ^{16}O

In the second beam test, which was carried out coinciding with the superconducting LINAC test, a 148 MeV ^{28}Si beam was used on ^{181}Ta target of 250 μg/cm^2 thickness (the effective energy of the beam on the target was only about 139 MeV, just above the Coulomb barrier, due to energy loss in the pressure window foil). A large fraction of the compound nucleus $^{209}Fr^*$ is expected to fission leaving a small percentage of evaporation residues (ERs) to survive and get transported through HYRA. Few steps of pressure settings were tried and at 1.25 Torr two peaks were clearly seen one centered at ~ 7 MeV and the other at ~ 9 MeV, with the lower energy peak yield of nearly 0.4 times that of the higher energy peak. The excitation energy of the compound nucleus, in this fusion reaction, is nearly 55 MeV and a 5n evaporation channel will lead to ^{204}Fr which then decays from the ground state with an emission of 7.03 MeV alpha particle with a half-life of 1.7 s and branching ratio of 80%. The ERs, produced with a mean energy of 18.1 MeV lose 0.6 MeV in half the thickness of the target and a further 3.9 MeV in the helium gas medium (1.25 Torr and 6.2 m long path). The ERs, with final energy centred around 13.6 MeV, will stop within 5 μm in the silicon detector. The alpha particle decay will be registered in the silicon detector with about 50% efficiency as the backward 2 π solid angle is not available for detection (7.03 MeV alpha particle needs nearly 40 μm of silicon to fully register its energy). Also it is seen from literature that for low energy heavy particles similar to these ERs, a pulse height defect (PHD) of more than 30 % is observed in silicon. Hence, from relative yield (~ 0.4) and energy (~ 7 MeV and ~ 9 MeV due to PHD of ~ 35%) arguments, we may infer that the two peaks possibly belong to the alpha decay and ERs. However, to be certain, we will need to correlate with position and timing information. The noise level in beam hall II needs to be reduced for better energy resolution and we require the complete focal plane setup for pixel position resolution. Work is on in the crucial detector and electronics development. We plan to take additional tests after incorporating the computer control of power supplies (to facilitate reproducible, faster setting of fields) and with possibility of position and timing information with reasonable resolution.

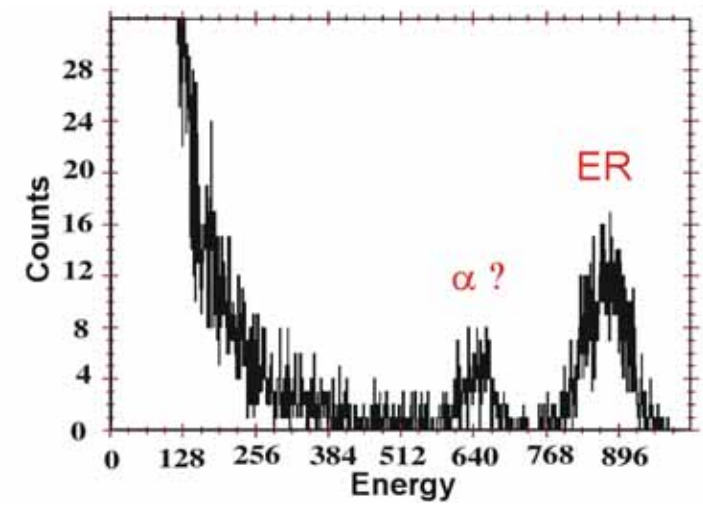

Fig. 3. Focal plane energy spectrum for $^{28}Si + ^{181}Ta \rightarrow ^{209}Fr^*$ system in gas-filled mode of HYRA first stage, at helium pressure of 1.25 Torr

Status of stage II :

As far as the second stage of HYRA is concerned, all quadrupole magnets, dipole (MD3) magnet and the power supply for MD3 are ready. The field mapping of the second stage magnets was carried out extensively at the vendor's (M/s. Danfysik) site (Fig. 4 (a) to 4 (d)).

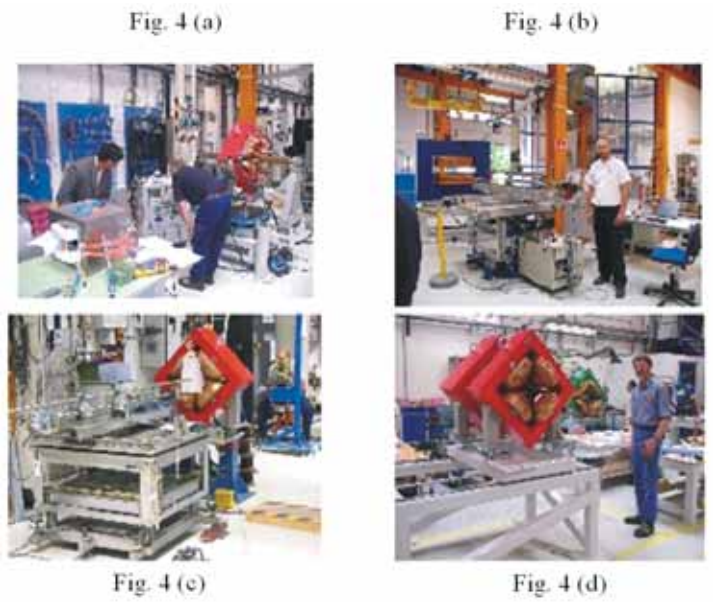

Fig. 4. Acceptance tests carried out at M/s. Dansfysik on HYRA stage II magnets; (a) harmonic content in quadrupole magnets using rotating coil method, (b) fringing field and homogeneous field measurements in dipole MD3 using hall probe, (c) effective length of quadrupole magnet using hall probe and (d) sideways movement check on Q6-Q7

All the relevant parameters for the electromagnets were subsequently extracted. The extracted effective lengths and integrated higher order components of some quadrupoles and the EFB angle of MD3 dipole are compared with design values in the table below.

Magnet	Parameter	Design Value	Measured Value
Q9	Leff	400 mm	401.5 (25%) - 405.2 (100%) mm
Q8	Leff	300 mm	306.4 (25%) - 301.55 (100%) mm
Q6	H.O. Comp.	< 1% of Bquad	< 0.2% of Bquad
Q7	H. O. Comp.	< 1% of Bquad	< 0.3% of Bquad
Q8	H. O. Comp.	< 1% of Bquad	< 0.3% of Bquad
Q9	H. O. Comp.	< 1% of Bquad	< 0.2% of Bquad
MD3	EFB Angle	12 +/- 0.5 deg.	12.02

Table 1: Comparison of measured and design values of HYRA stage II magnets

The sideways movement option of Q6-Q7 was tested for reproducibility. This option will provide enough space for the use of auxiliary detectors at the focal plane of HYRA, in gas-filled mode, to carry out isomer decay studies.

The power supplies for the second stage quadrupole magnets, developed by Beam Transport Group, are being assembled in the cabinets designed and fabricated for this purpose (Fig. 5).

Fig. 5(a)

Fig. 5(b)

Fig. 5. (a) Cabinets for the assembly of high current, highly stable power supplies for quadrupoles Q6 to Q9 and (b) one of the partially assembled power supply.

Superconducting Q1-Q2:

Development of superconducting Q1-Q2 is in progress, with major efforts from cryogenics group at the centre. The pole and yoke of the superconducting Q1-Q2 doublet are ready and have arrived. The wire winding machine has been fabricated (Fig. 6a and 6b) and tested by winding a 1 mm thick copper wire using the aluminum formers (Fig. 6c) made to mimic the poles and yoke. Minor adjustments were done to perfect the winding process and a trial winding of copper dipped in epoxy (Fig. 6d) has subsequently been carried out. After few more successful trials with epoxy coated copper wire, we will be carrying out the actual coil winding with superconducting wire for both Q1 and Q2. The final design of the cryostat will be taken up shortly after the coils are mounted.

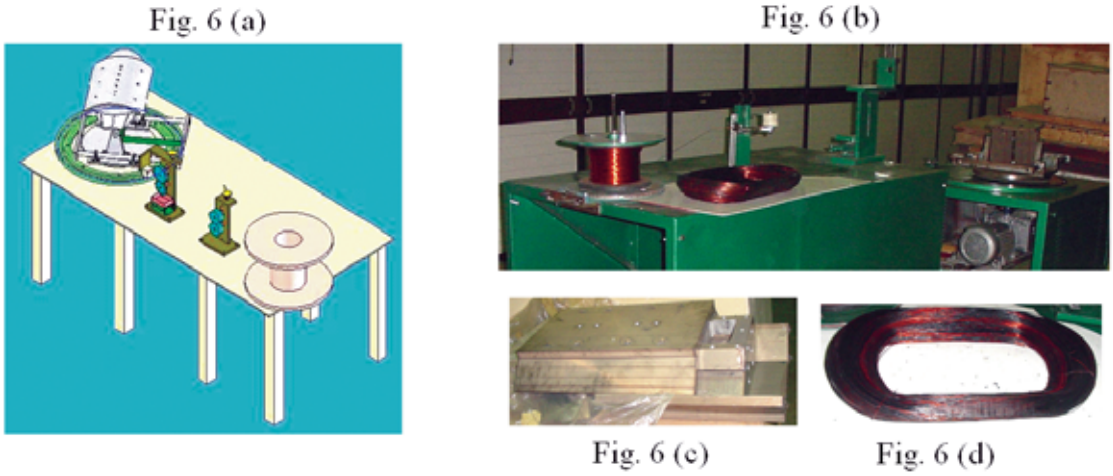

Fig. 6. (a) Design and (b) actual wire winding machine for superconducting Q1-Q2 coils along with (c) aluminum former and (d) the epoxy coated copper coil

The electrostatic dipole (ED), which is a crucial element in the second half of HYRA needs funds (compensating for increase in foreign exchange and customs duty incurred so far). The funding agency has been requested to provide the same and adequate time to realize the fabrication of ED and the same was put forward to a committee along with progress report, recently.

The transmission efficiency of HYRA in gas-filled mode has been simulated for various separator/detector configurations. These are explained and tabulated in detail, for the systems studied during the beam tests, in section 4.3.3. Further tests with gas-filled mode operation will be taken up from mid-2007, after completing the remote control system for the power supplies.

4.3.3 Estimation of transmission efficiency of gas-filled mode of HYRA

S. Nath and N. Madhavan

The HYbrid Recoil mass Analyzer (HYRA) [1], being commissioned at IUAC, will

have two modes of operation viz. gas-filled mode and vacuum mode. The electromagnetic configuration of HYRA in the gas-filled mode is Q1-Q2-MD1-Q3-MD2-Q4-Q5, where Q and MD stand for quadrupole magnet and dipole magnet, respectively. Provisions are kept to place the focal plane detector either at the end of Q5 or after MD1 for which provision of side-ways movement of Q3 is incorporated. At present, HYRA is commissioned up to MD2 (with normal quadrupole doublet Q5-Q4 in place of Q1-Q2) and the focal plane detector placed right after. In future, a superconducting quadrupole doublet Q1-Q2, which is being developed, will be placed immediately after the target and the whole layout will be completed.

In this report, we present the results of a Monte Carlo based calculation for the transmission efficiency of HYRA in gas-filled mode. The evaporation residues (ERs) produced in a complete fusion reaction will have broad distributions in angle, energy and charge state. ERs, when subjected to collisions with the gas molecules inside the separator, will attain charge state and velocity focusing. These will lead to enhanced collection efficiency while sacrificing mass resolution at the focal plane. The ERs, on their journey towards the focal plane detector will lose energy continually and their charge state also will change. We calculate the angular, energy and charge state distributions of the ERs by a semi-microscopic Monte Carlo code [2]. Individual ion trajectories are calculated using first order transfer matrices [3]. Energy loss of the ERs in the gas-volume (helium at ~1.0 torr pressure in our case) is calculated [4] in steps of 1.0 cm. Charge state of the ERs as a function of its velocity (energy) and atomic number is calculated [5] at each step. This algorithm has been found to reproduce calculated/measured transmission efficiencies for DGFRS at Dubna [6]. Calculated transmission efficiency of HYRA in the present configuration for two systems is shown in the table below assuming size of the focal plane detector to be 10 cm × 5 cm (or 5 cm x 5 cm within brackets).

System	**Beam energy (MeV)**	**Target thickness (μg/cm2)**	**Efficiency [%]**	
			Detector after MD1	**Detector after MD2**
$^{16}O+^{184}W$	100	210	17.6 (9.3)	8.0 (4.4)
$^{28}Si+^{181}Ta$	140	200	37.4 (33.2)	35.5 (28.2)

These numbers, which are specific to a particular reaction, are the upper limits for efficiency which need to be compared with measurements. In the case of $^{28}Si+^{181}Ta$, the increased efficiency is mainly due to larger kinematic focusing. The larger gaps chosen for the dipoles MD1 and MD2 (120 mm) and larger apertures chosen for quadrupoles (200 mm diameter) allow better transmission of ERs in HYRA though the flight path is longer. The use of MD2 in gas-filled mode in addition to MD1 will further reduce the background at the focal plane. With the commissioning of superconducting Q1Q2, which are planned to be of half the length but nearly thrice the pole-tip

field as that of present normal (room temperature) quadrupole doublet (Q5-Q4), we expect efficiency to go up further for all systems.

The trajectories, through HYRA, of the ER, ^{205}Fr from ^{28}Si (140 MeV) + ^{181}Ta (~ 0.2 mg/cm^2) $\rightarrow$ ^{209}Fr* $\rightarrow$ ^{205}Fr + 4n are shown in Fig. 1 (a) and (b) for the dispersive and vertical planes, respectively. The detector, placed right after MD2 is of the size 10 cm (X) x 5 cm (Y).

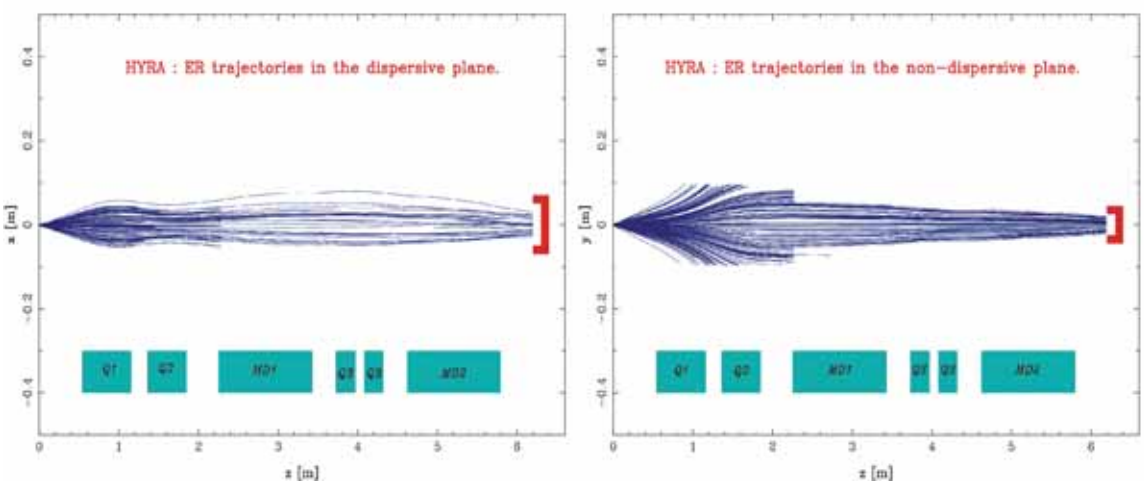

Fig. 1. Typical trajectories through HYRA for one type of ERs, ^{205}Fr formed in ^{28}Si (140 MeV) + ^{181}Ta (~ 0.2 mg/cm^2) shown in (a) dispersive plane (a) and (b) vertical plane respectively.

REFERENCES

[1]. N. Madhavan et al., Proceedings of the DAE-BRNS Symp. on Nucl. Phys. 51 (2006) 636.

[2]. S. Nath, submitted to Nucl. Instr. and Meth. A (2007).

[3]. H. Wollnik, Optics of Charged Particles (Academic Press, Orlando, 1987).

[4]. J.F. Ziegler et al., The stopping and range of ions in solids, Vol. I (Pergamon Press, Oxford, 1984).

[5]. Yu. Ts. Oganessian et al., Supplement to Z. Phys. D 21 (1991) S357.

[6]. K. Subotic et al., Nucl. Instr. and Meth. A 481 (2002) 71.

4.4 MATERIALS SCIENCE FACILITY

A. Tripathi, Ravi Kumar, V.V. Shivkumar, F. Singh, S.A. Khan, P. K. Kulriya, I. Sulania, R.N. Dutt, P. Barua, A. Kothari and D.K. Avasthi

The materials science facilities continue to support the research programs of a large number of users from different universities and institutions from India and abroad. The swift heavy ion irradiation related experiments are performed in the three chambers in the beam line as well as in the general purpose scattering chamber. Besides this, the off-line facilities are also being used by

many users for preparing and characterizing samples. A total of 101 user experiments comprising more than 300 shifts were performed this year, without any beam time loss due to major facility break down. Experiments are being done in different areas of swift heavy ion induced materials modification and characterization and the details of the research programs are given in Section 5.2

The high vacuum chamber in materials science beam line is used in most of the experiments for irradiation and ERD studies. A new vacuum controller and extra gauges were installed in the beam line this year for smoother operation. The goniometer chamber mounted on UHV chamber for channeling studies had developed a problem and efforts are on to rectify the problem.

FTIR system Nexus 670 from Nicolet is being actively used for vibrational analysis of thin films as well as bulk materials by users with analysis of more than 700 samples from 30 users was undertaken. The PL/IL study of more than 350 samples from nearly 25 users was also done this year.

4.4.1 Irradiation Chamber in BH II

A. Tripathi, R. Ahuja, R.N. Dutt, P. Kulriya, F. Singh, S.A. Khan and D.K.Avasthi

The chamber was aligned and integrated to the beam line last year. The problems faced in the first beam test were sorted out and another test run was taken. The alignment of the irradiation chamber, 1 mm entrance slit and XRD chamber were re-done. Alignment was repeated with chamber in vacuum. A cross mounted in the beam line for mounting C-foil for facilitating experiments with equilibrium charge state. During the test experiment the automated ladder control was used.

Fig. 1. The beam line with cross for equilibrium charge state studies mounted

The in-situ XRD facility set up in this beamline was tested last year. The facility has been used in the study of the kinetics of the growth of nanoparticles under 90 MeV Ni ion irradiation. The details are given in section 5.2.

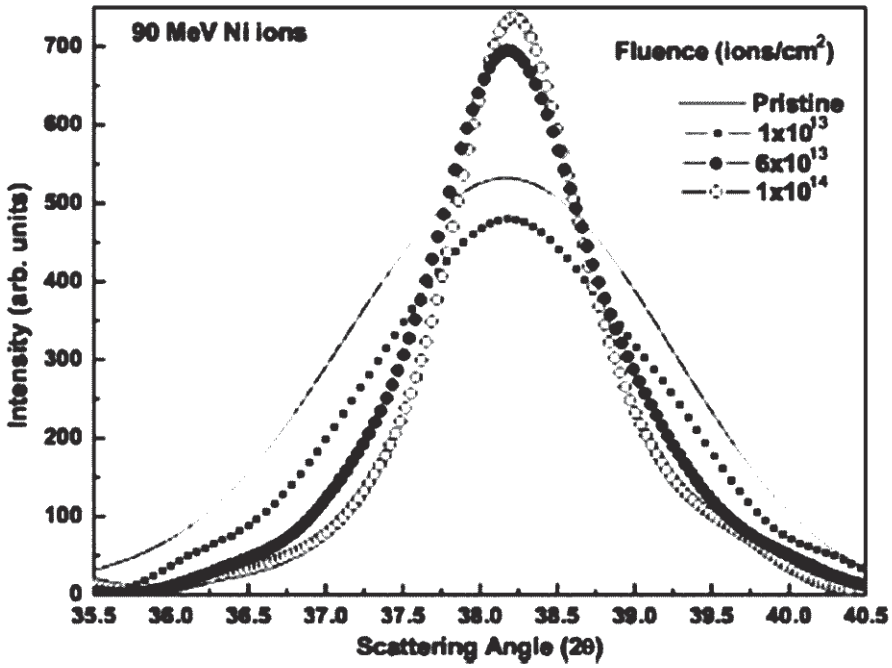

Fig 2. In situ X-ray diffraction spectra of the pristine and irradiated samples with increasing fluence [1]

REFERENCE

[1.] Y.K. Mishra et al, Appl. Phys. Lett., 90, 073110 (2007)

4.4.2 Scanning Probe Microscope

A. Tripathi, I. Sulania

Multi Mode SPM with Nanoscope IIIa controller acquired from Digital/Veeco Instruments Inc. was extensively used in all the modes in user experiments. The areas of research include: Ion induced surface morphology, SHI induced changes in size and its distribution of nanoparticles, SHI induced modification in magnetic domains, SHI induced plastic flow of material and Characterization of ion tracks in terms of size and number density. All SPM modes were used in experiments this year: AFM, MFM, C-AFM, STM, STS and F-d mode etc. PSD studies for surface growth and Force-Distance studies were initiated this year. An arrangement for MFM study with applied field was also developed. This year more than 800 samples from 60 users have been studied. An illustartive example of the evolution of dot structure with increasing angle of incidence on 1.5 keV Ar irradiation of InP surface is shown in figure 1. The detailed results obtained are discussed in materials science research section 5.2.

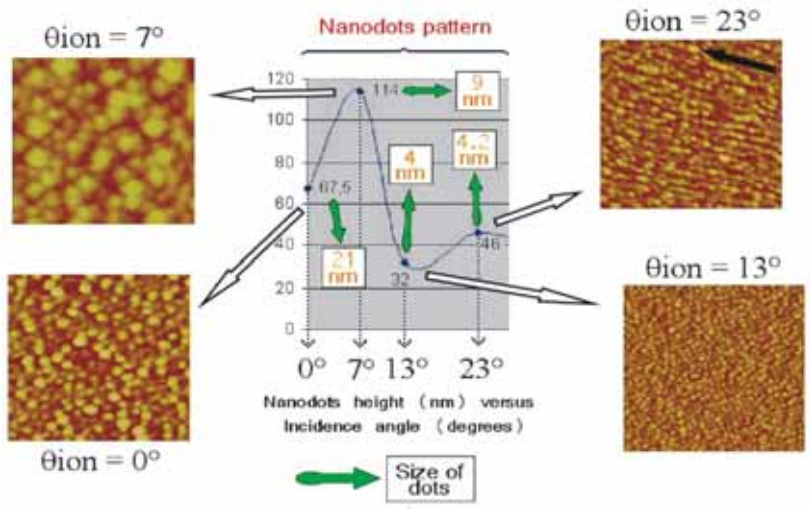

Fig. 1. The evolution of dot structure with increasing angle of incidence on InP surface after irradiation with 1.5 keV Ar atoms

4.4.2.1 Development of an Electromagnet for Magnetic Force Microscope

A.Tripathi, I. Sulania, A. Mathur*, O.P. Sinha* and D.K. Avasthi

*Amity University, Noida

An electromagnet with field up to 500 gauss field for use with MFM has been developed. The details are given in Section 5.2. A photograph of the magnet is shown in Fig 1. Fig 2 shows a measurement using the magnet where the direction of the applied magnetic field is along the sample surface and the field aligns the domains along the field direction.

Fig. 1. Electromagnet mounted on MFM

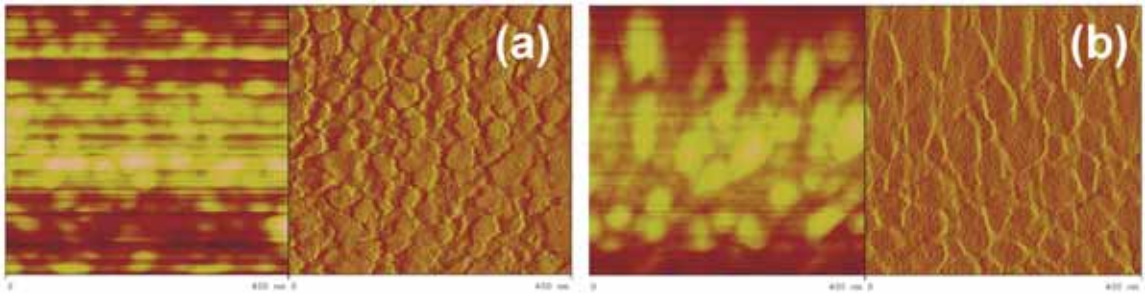

Fig 2. MFM igage (a) without and (b) with applied magnetic field

4.4.3 Installation and testing of micro-Raman setup in beam hall-II

Fouran Singh, A. Tripathi, Y.S. Katharria, Amit Kumar, D. K. Avasthi

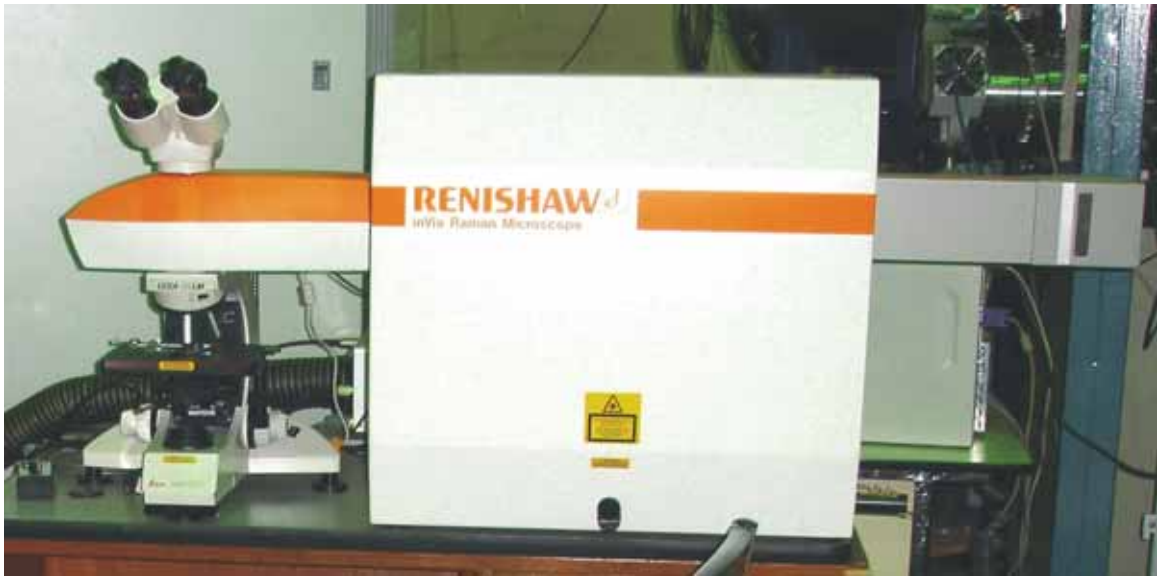

Fig. 1. Renishaw InVia Raman Microscope

We have acquired an InVia Raman microscope from Renishaw UK. This setup has been installed and tested offline in the beam hall-II. The system consists of Ar ion laser with 514.5 nm wavelength and 50 mw power. The Microscope is shown in fig 1. The microscope has very high sensitivity integrated components which enables high resolution confocal measurements. Setup can also support multiple lasers, with automatic software switching of excitation wavelength. Exceptional sensitivity for ultra-low signal detection with minimum noise is possible with compact RenCam CCD detector (105 mm x 105 mm x 135 mm). It is thermoelectrically cooled and operates at -70 °C without the need for additional cryogenic coolants and it is deep depletion with UV enhanced coating for future UV excitation applications. The detector is sensitive from 100 to 3200 cm^{-1}. The lower limit is set by the notch filter used for suppressing the Raleigh background of

laser. Setup is also equipped with;

a) WiRE™ 2.0 software for intuitive operation and data manipulation.

b) High stability honeycomb base-plate with precision kinematic mounts for easy laser swapping.

c) Automatic alignment optimization with built-in system performance validation.

d) Automatic capability for switching to confocal operation.

The installed, aligned and calibrated setup has been tested for its performance on Si as shown in fig 2(a) and then on pristine and 60 MeV Ni ion irradiated MWCNTs as shown in fig 2(b). Setup has been used for the characterization of various kinds of samples like Si, In P, ZnO, C_{60}, C_{70}, CNT, SiC etc. This setup will be integrated with beam line of LINAC accelerator for studying the in-situ modifications of materials under SHI irradiations.

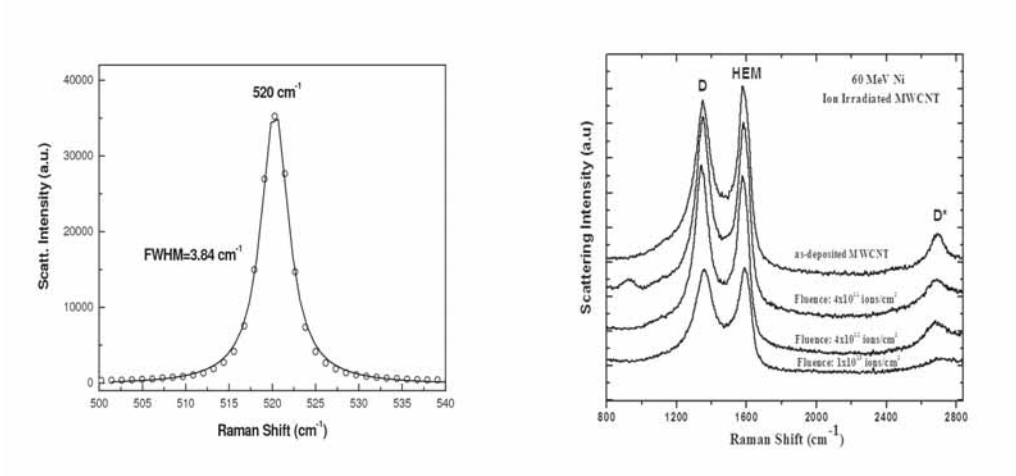

Fig. 2. Raman spectrum for (a) Si (b) MWCNT after irradiation with 60 MeV Ni

4.4.4 Experimental setup for the investigation of depletion and sputtering induced by swift heavy ions

Saif A. Khan, M. Kumar[1], D. K. Avasthi, I. Sulania, A. Tripathi, F. Singh and A. Kumar

[1]Department of Physics, University of Allahabad, Allahabad -211 002

Swift heavy ions (SHI) are known to produce loss of elements like hydrogen and nitrogen, and produce electronic sputtering in a variety of materials. These phenomena have been utilized to understand the mechanism of ion-solid interactions. Elastic recoil detection analysis (ERDA) facility exists in the centre for over a decade which indirectly gives quantitative information of the lost elements in the studied materials. However, the information about the ejected species particularly about the cluster emis-

sion could not be derived. Also, the information related to charge carried by these ejectiles was missing. To get answers to these questions, an experimental apparatus based on quadrupole mass spectrometer (QMS) has been setup in the materials science beam line. Below we present the experimental setup description and some preliminary test results.

The QMS is attached to a 90° port of ultra-high vacuum (UHV) chamber. It collects ejected species from the samples which are tilted at an angle of 20° with respect to beam direction. The probe consisting of 3 lens optics is nearly 5 mm from the sample surface during the measurements. The QMS instrument (QMG 422 with SIMS option from Pfeiffer) operates at 2.25MHz and can mass analyze in the range 1-1024 amu with mass separation ($\Delta M/M$) better than 0.01.

The UHV chamber, pumped by a turbo-molecular pump and an ion-pump, has a base pressure of the order of 10^{-9} mbar. However, during experiments with SHI beams the pressure in the chamber is only of the order of 10^{-7} mbar due to the coupling of the chamber with high vacuum chamber which precedes it in the beam-line. There is a load lock system, evacuated by a separate turbo-molecular pump, to introduce samples in the main chamber without disturbing its vacuum. A wide primary beam is used in order to obtain a more uniform distribution of ion current on the tilted sample. There is a provision to bias the spectrometer with respect to the sample in order to collect the charged ejected species more efficiently. Total ions falling on the sample can be determined by calibrating ladder current with suppressed faraday cup in the beam line. The data can be recorded either for selected mass numbers or for selected mass range with the help of the software provided by Pfeiffer.

The first experimental tests carried out were to monitor ejected species from fullerene and halide thin films by 100 MeV Ag ions. We present here the result of barium fluoride sputtering studies. We had earlier determined its sputtering yield by online-ERDA technique. In the test experiment, we tried to find out which species are ejected out and whether they are negative, positive or neutral. First, we collected data for 1-200 amu mass range and identified the ejected species in each of the negative, positive and neutral modes of collection. Finally, we recorded data for these species only so as to get the detection rate (counts per second) vs. fluence curve for each of them.

Table 1. List of detected species in different modes during sputtering of BaF_2

Detection mode	Detected species
Neutral species	F_2, BaF, F
Negative species	F
Positive species	Weak signal of Ba

For the case of barium fluoride, the Table 1 gives the fragments detected in the three detection modes. Collection of BaF and F implies that there are ejection of heavier species and even BaF_2 which may have got fragmented in the used neutral mode of detection. However, we did not observe BaF_2 as such with the experimental sensitivity.

The experimental apparatus described above will enable measurement of ejection processes occurring during SHI irradiation and the effect of ion energy, ion fluence and its charge state on the process. The detailed analysis of the ejection process may give an insight into the fragmentation process occurring due to SHI and the indirect determination of the size damaged zones produced by each impinging ion.

4.4.5 RF sputtering and ball milling systems

V.V.Siva Kumar

The rf sputtering system was made operational after carrying out many works some of which are; provision for rotary pump exhaust to be let into atmosphere, earthing of the system, gas flow connections, replacement of roughing valve, solving RFI problems, leak testing and rectification of leaks. The rf sputtering system was used to grow thin films of Fe-PI (MS University, Baroda) and ZnS/SiO_2 (Allahabad university) and for deposition of thin film using rf plasma by vacuum evaporation of aniline liquid monomer (JMI, New Delhi).

The ball milling system was in operational condition and one user (University of Rajasthan) work was done.

4.4.5.1 Development of microwave plasma based deposition system.

V. V. Siva Kumar, M.Archunan, P. Barua and D. K. Avasthi.

This year, the gas flow and pressure control components were connected to the deposition chamber and tested at pressures in which thin film depositions are done. The roughing line, backing line, gate valve, Turbo pump and Scroll pump were integrated to the chamber and gate valve interlock with Turbo pump was done. Provision for scroll pump exhaust to be let into atmosphere was made. A high vacuum of 4×10^{-6} torr was produced in the chamber. Other works required for producing the microwave plasma are in progress.

4.4.6 Development of temperature dependent automated dielectric measurement setup

Shailendra Kumar[1], Ravi Kumar, S. K. Saini

[1]Department of Applied Physics, Aligarh Muslim University, Aligarh-202002

Multiferroic materials are simultaneously ferromagnetic and ferroelectric. They have the potential for applications in magnetic as well as ferroelectric devices and also used in giant devices

like electrical transformers to tiny devices like sensors, integrated circuits and storage devices. All these require accurate measurements of temperature and frequency dependent dielectric characteristics. The dielectric constant as a function of temperature is a unique property to know the transition temperature of ferroelectric materials. The dielectric measurement setup was developed in view of these requirements.

The main objective of the design of cryostat (see fig.1) and automation of the dielectric setup is to the study the characteristic of the High-Dielectric and ferroelectric materials. The aim is to provide a compact dielectric set up to the researchers at IUAC, New Delhi, with minimum complexity with accurate and reliable measurements. For measuring dielectric constant of ferroelectric materials as well as high dielectric materials, a liquid nitrogen (LN_2) dipstick has been designed. In this cryostat we can carry out following measurements:

1. Frequency (75 kHz - 30 M Hz) dependent dielectric properties.
2. Temperature (80 K - 500 K) dependent dielectric properties.
3. Temperature (80 K - 500 K) dependent CV and IV measurements.
4. Impendence, Inductance and resistivity can also be in the temperature range 80 K -500 K.

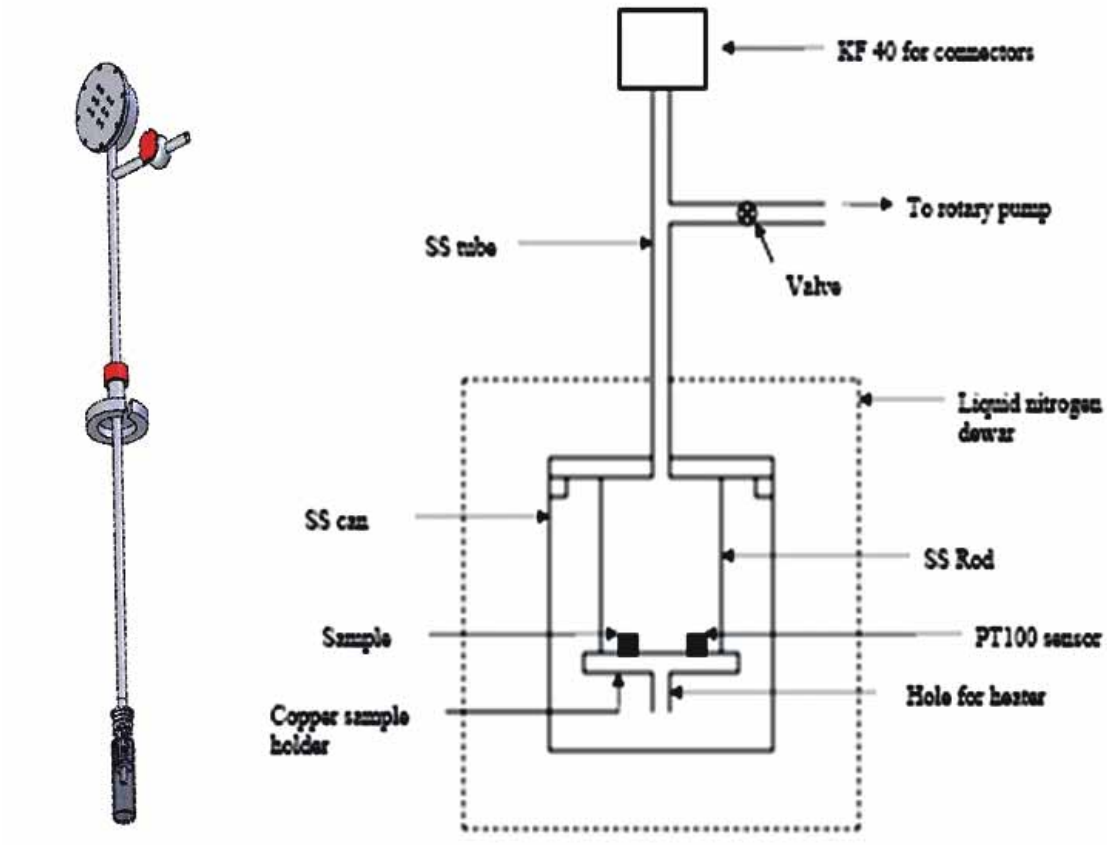

Fig.1. Schematic diagram of the cryostat

A calibrated PT100 temperature sensor is placed near to the sample on the copper plate. A 50 W heater of LakeShore has been inserted in the hole at the base of copper plate. The whole of this sample holder is enclosed by removable ss cup. When this dipstick cryostat is inserted inside the LN_2 dewar, this cup kind of attachment is kept under rough vacuum using a rotary pump. There are ten electrical connections: four for sample, four for sensor and two for heater. Four shielded coaxial cables give out the electrical connections of the sample. This electrical connection travels through the thin SS tube which is about 1 meter in length. All ten connections end as a ten vacuum compatible female BNC connector and then six (four sensor and two) connections terminate in a special D-type male connector through six male BNC connector from the KF-40. There is sufficient and ample space to keep the samples for the measurement. The sample can be electrically connected using silver epoxy. The temperature of the sample is controlled using the LakeShore temperature controller (Model 340) and stabilized within 50 mK. This setup is fully automated using standard NI interfacing. The interfacing program has been written using LabView software.

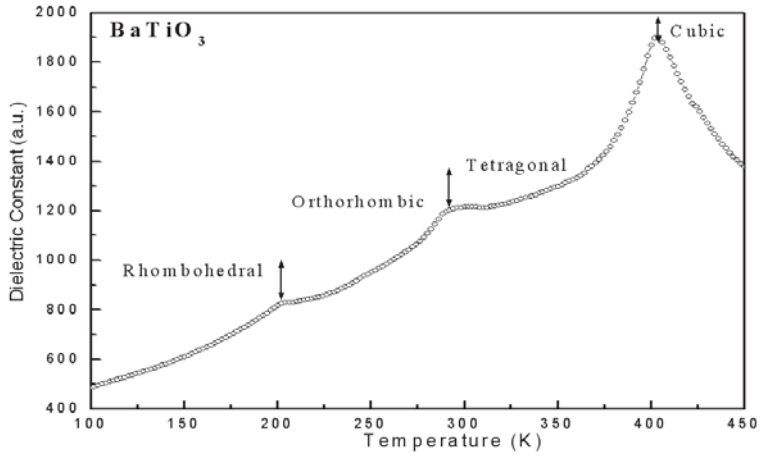

Fig.2. Temperature dependent dielectric constant (e) at 100 kHz for $BaTiO_3$

Typical dielectric measurements carried out

Fig. 2 shows the variation of the dielectric constant with temperature for $BaTiO_3$ at 100 kHz. It is clear from the Fig.2 that $BaTiO_3$ exhibits all three ferroelectric transitions.

4.4.7 Low temperature sample cooling unit with in-situ X-ray Diffractometer

P. K. Kulriya, R N Dutt, Amit Kumar, R Ahuja, A. Kothari, A. Tripathi and D. K. Avasthi

The in-situ XRD (Model D8 Advance) was integrated to the beam line and in-situ testing was completed last year. This year a sample cooling unit with Lakeshore 340 temperature controller was designed and fabricated for in-situ XRD system.

The low temperature cooling unit was fabricated at work shop of the IUAC. The cooling unit consists of liquid nitrogen (LN_2) cooling line, bellow, LN_2 reservoir and copper sample holder (Fig 1). The LN_2 cooling line is made of double walled stainless steel pipe. One end of this pipe was connected to the copper reservoir via a stainless steel bellow. The LN_2 is filled in this assembly from the top side. The LN_2 reaches to the reservoir through the pipe, right behind the sample holder. The vacuum around the LN_2 line was achieved with existing vacuum unit attached to the XRD system. The reservoir passes through the vacuum jacket through a port and makes contact with sample holder which enables cooling of sample holder when LN_2 is filled.

The sample holder is made up of copper block, on which a heater (50W, 50 ohms) and a temperature sensor (Pt100) are mounted. The sensor is fixed reasonable close to the sample. The heater is also mounted close to the temperature sensor in order to minimize the delay. The temperature of sample was controlled by Lakeshore 340 temperature controller.

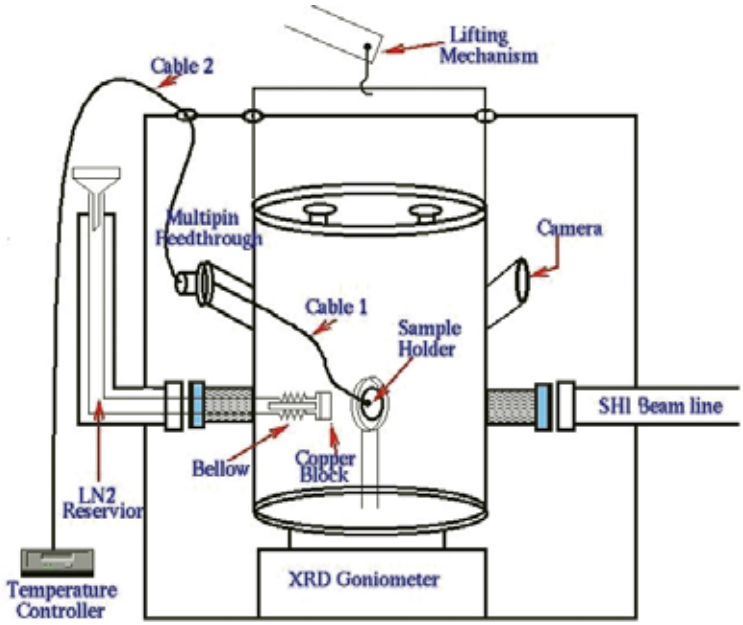

Fig.1. Schematic of low temperature sample unit for in-situ X-ray diffractometer

Testing of sample cooling unit

The system was tested with LN_2 and a temperature of 103 °K was achieved. The thin film of C_{60} (thickness = 50nm) prepared by evaporation, was used for testing of sample cooling unit. The GAXRD spectra at glancing angle 2°, from a range of 2-theta from 8° to 25° with an increment of 0.02° was recorded at different temperature 200 °K, 255 °K and 300 °K (Fig 2). The XRD data was analyzed with PowderX software. It shows that C_{60} film has cubic phase at room temperature with a lattice constant a =14.171 Å. When sample was cooled at T= 255° K, then its lattice constant decreased a = 14.132 Å. It shows that there is a phase transition from cubic lattice to fcc lattice around T= 255 °K. If the temperature is further reduced then there is negligible change in lattice constant and system remain in fcc phase.

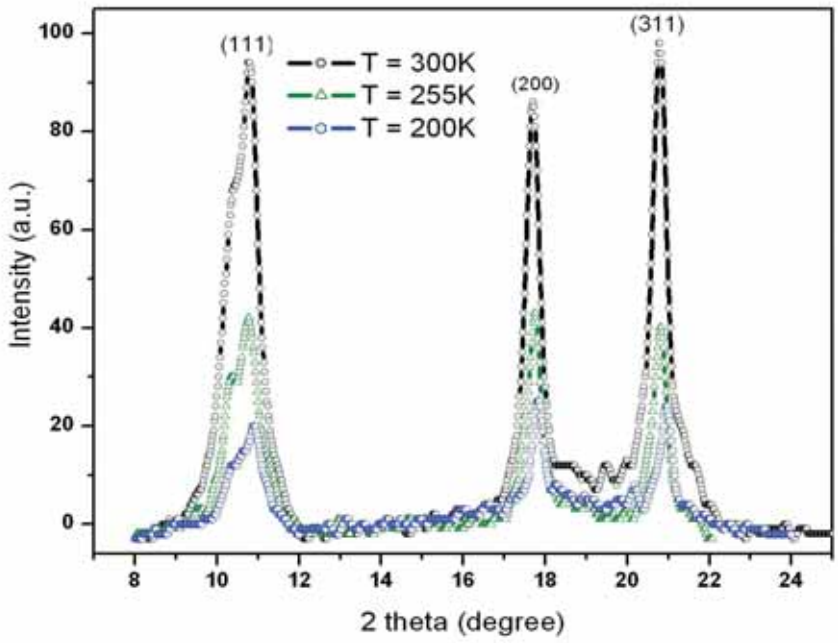

Fig: 2 Low temperature XRD spectra of C_{60} thin film (t = 50 nm) recorded at different temperature 200 °K, 255 °K and 300 °K

4.5 RADIATION BIOLOGY

4.5.1 Status of the Radiation Biology Beam line

A. Sarma, P. Barua, A. Kothari, E.T. Subramaniyam, M. Archunan

The specially designed beam line can deliver beams of proton, ^{7}Li, ^{11}B, ^{12}C, ^{14}N and ^{16}O. The flux can be controlled from 10^2 particles/sec/cm^2 to 10^6 particles/sec/cm^2. The exit window is having 40 mm diameter with active area for cell irradiation defined by the standard 35 mm petri-dish. The uniformity is better than 97%. The flux control is done by adjusting a double slit through CAMAC from control room. A preset controller for faraday cup ensures the exposure repetition as per user requirement.

A major redesigning of the irradiation system is currently going on, which would take care of the remote handling of petri dishes in an enclosed sanitised environment during irradiation, multiple irradiations of one sample after another without losing time. This allows to keep the petri-dishes in the medium when they are not being irradiated. The dosimetry system would also be improvised along with that. The renovation would facilitate better experimental condition from the biological point of view.

The components for the irradiation system have been procured and the process of installation as well as additional support system fabrication has started.

4.5.2 Status of the Molecular Radiation Biology Laboratory

A. Sarma

The laboratory is designed to extend user support to the best possible way during experiments. The experiments that are undertaken recently require suitable in-house facilities for relevant protocols. Apart from the equipments of the Cell Culture facility like autoclave, biosafety cabinet, CO_2 incubator, and other normal equipment like microbalance, oven, refrigerated centrifuge, PCR machine, Gel Doc, AFIGE system and Semi dry transblotter etc., we have installed a -80°C Ultra Freezer [Heto] and a -20°C Deep Freezer [Vest Frost]. In addition, a fluorescent microscope [Carl Zeiss] has been installed to facilitate the experiments based on FISH and immunofluorescent assays.

For accurate cell counting, a Coulter Cell Counter [Beckman Coulter] is installed in the laboratory. This equipment would drastically enhance the speed and accuracy of post irradiation cell plating during the beam time and thus save a lot of time.

4.6 ATOMIC PHYICS BEAM LINE

4.6.1 Status of Atomic Physics Beam Line

Rewa Ram, S.K. Saini, Ranjeet K Karn, B.P. Mahanty[1], and T. Nandi

[1]Department of Physics, Punjabi University, Patiala - 147 002

The beam line up to the vacuum chamber was installed in the beam line at 10 east and checked the alignment with beam. Top lid of the chamber was to move up and down using a screw-motor system. This was malfunctioning and we replaced it by a hydraulic lifting system. Further, different axis of the target ladders in the triple axis target manipulator was revamped by using a rack and pinion gear system. In this chamber we have installed a precision foil thickness measuring set up. This beam line is planned to carry out several experiments such as beam-foil, inner-shell ionization, and electron spectroscopy in the vacuum chamber and at the back charge state fraction (CSF) analysis of the beam on passage of the solid foil. CSF measurements will be done using electrostatic analyzer and position sensitive parallel plate avalanche counter (PSPPAC). The beam line is designed in such a way that one set up does not disturb the other. Tapered vacuum chamber for CSF measuring set up and retractable Faraday cup are being fabricated in our work shop and beam slits have been ordered. We will be able to install the entire line in this year. PSPC (Position sensitive proportional counter) developed for the Doppler Tuned Spectrometer (DTS) project at general purpose scattering chamber (GPSC) is ready to be used for the DTS experiments. Off line test results of this are high lighted below.

4.6.2 One Dimensional Position Sensitive Proportional Counter for DTS setup

Ranjeet K Karn, Rewa Ram, Anjan Datta[1], C.P. Safvan, A. Roy and T. Nandi

[1]Department of Physics and Astrophysics, Delhi University, Delhi- 100 007

Development of instrumentation to measure the intensity, energy and position of x-rays has been a major area of investigation within experimental physics over many decades. The ability of the gas proportional counter to record incident particle or x-ray photon intensity with only a very small amount of primary charge produced, is a unique feature of the detector. Doppler Tuned Spectrometer, requires a detector which has good position resolution, good integral linearity, high efficiency and sufficiently large collection area. The one dimensional backgammon type position sensitive proportional counter has met most of the required criteria.

The design of the detector is based on the principle of charge division, due to its simplicity in design, good position resolution, good integral linearity and high counting efficiency. The detector consists of three main parts, the housing, the window plate and the detector mounting plate. Detector housing is a SS chamber of 200x50x50 mm and both window plate and mounting plate fit over it gas tightly. Window plate has a window of 170 x 2.5 mm and it supports mylar foil over it. The interior of the detector is filled with an argon (90%) and methane (10%) gas mixture (P10) and sealed with O-rings at the entrance and rear ends. An x-ray photon enters the detector through a 20 μm thick mylar foil. These photons interact with the gaseous atoms and ionize them. The detector mounting plate consists of two SHV connectors at the ends and two limo connectors in between. The tip of the SHV connectors hold a 30 μm diameter Gold plated tungsten wire, which serves as anode.

Design of cathode is crucial because it will ultimately provide the desired position resolution. Cathode is made of a copper deposited rectangular printed circuit board of 148 x10 mm and has a diagonal insulating line of 500 μm thick. The two triangular cathodes provide two cathode signals, the ratio of which leads to the position information. The detector is operated in the proportional region. The charges collected at the cathodes are sent to charge sensitive preamplifier (Ortec 142 PC). The active region i.e., the distance between cathode and anode was kept 7 mm.

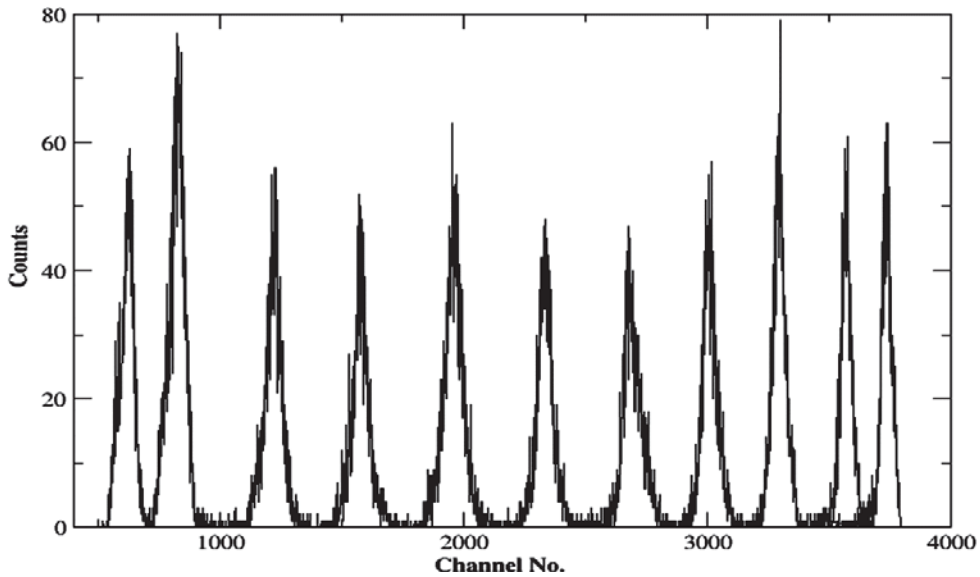

Fig.1. Spectra taken with a mask of hole 1mm with 5.9 keV ^{55}Fe source at positions 0, 15, 30, 45, 60 and 69 mm from one end

To test the detector we exposed it to a 55Fe x-ray source collimated with one mm wide slit. Proper bias voltage in the proportional region was selected by optimizing the signal in whole length of the detector. Optimize voltage was 1740V. For position resolution and linearity the source was moved along the x-direction to another location by known distance. This process was repeated to a number of times to cover the full length of the detector and an array of data points was collected. This produced a one dimensional array of peaks shown in Fig.1.The position resolution varies 1.113 mm at center to 1.360 mm at end.